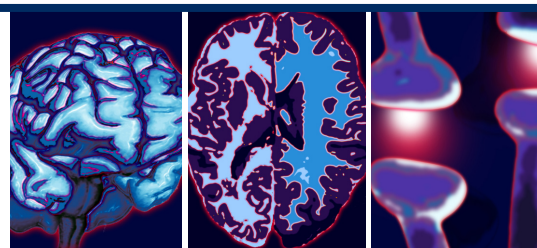# Neuropsychiatry and quantitative EEG in the 21st Century

Robert W Thatcher[†]

Practice points

- Use conventional clinical evaluation to derive a diagnosis and identify patient symptoms.

- Measure eyes open and eyes closed artifact-free quantitative EEG.

- Calculate auto- and cross-spectra to identify scalp locations and network deviations from normal.

- Use EEG tomography to link the patient's symptoms and complaints to functional systems in the brain.

- Identify and separate the 'weak' systems from compensatory systems.

- Use Z-score biofeedback to target the deregulated brain subsystems to reinforce optimal and homeostatic states of function while the clinician monitors the patient's symptom reduction.

- Use quantitative EEG to evaluate pre- versus post-treatment and follow-up evaluations to determine treatment efficacy (e.g., medications, repetitive transcranial magnetic stimulation, electroconvulsive therapy, brain–computer interfaces and biofeedback, among others).

SUMMARY The human brain weighs approximately 3 lbs and consumes 40–60% of blood glucose. This disproportionate amount of energy is used to create electricity in approximately 100 billion interconnected neurons. Quantitative EEG is a real-time movie of the electrical activity of the preconscious and conscious mind at frequencies of approximately 1–300 Hz. Numerous studies have cross-validated electrical neuroimaging by structural MRI, functional MRI and diffusion spectral imaging and thereby demonstrated how quantitative EEG can aid in linking a patient's symptoms and complaints to functional specialization in the brain. Electrical neuroimaging provides an inexpensive millisecond measure of functional modules, including the animation of structures through phase shift and phase lock. Today, neuropsychiatrists use these methods to link a patient's symptoms and complaints to functional specialization in the brain and use this information to implement treatment via brain–computer Interfaces and neurofeedback technology.

[†]Author for correspondence: NeuroImaging Laboratory, Applied Neuroscience Research Institute, St Petersburg, FL 33722, USA;
Tel.: +1 727 244 0240; rwthatcher@yahoo.com

future medicine fsg
part of

EEG is the measurement of the brain-generated electrical potential between locations on the scalp and/or with respect to a reference. Quantitative EEG (qEEG) invovles the use of computers to precisely quantify electrical potentials of approximately 1–300 Hz, representing subsecond measures of summated local field potentials generated in groups of cortical pyramidal neurons [1]. In the last 40 years, over 90,000 qEEG studies have been listed in the National Library of Medicine's database [201]. To review this vast literature, it is best to use the search terms 'EEG and x' where 'x' is a topic such as schizophrenia, dyslexia, attention deficit, reliability, validity, obsessive–compulsive disorders, evidenced-based medicine, anxiety or phobia, among others. A reading of the studies and abstracts shows that the vast majority of these studies are qEEG studies involving computer analyses (e.g., spectral analyses, ratios of power, coherence or phase, among others). The search term 'EEG' and not 'qEEG' is necessary because the National Library of Medicine searches article titles/abstracts, and these rarely if ever use the term 'qEEG' in the title (e.g., this author has published six books and over 200 total publications and never used the term 'qEEG or QEEG' in the title or abstract). This is why a small 'q' is used in this paper to emphasize that the summation of electrical potentials generated by pyramidal neuron synapses are the sources of the EEG and the 'q' designates quantification as opposed to 'eye-ball' or visual examination of the EEG traces or squiggles without quantification as used in clinical routine. This article is written with a special emphasis on the use of qEEG after visual examination by psychiatrists, neuropsychiatrists, clinical psychologists, psychologists, neuropsychologists and neuroscientists who are the primary users and publishers of psychiatric-related articles using qEEG.

Historically, visually recognized EEG patterns and other electrophysiological measures (evoked potentials and event-related potential) were used to discern etiological aspects of brain dysfunction related to psychiatric disorders with reasonable success, but not at the level that qEEG can be used as a standalone diagnostic method for psychiatric disorders [2]. Instead, qEEG was used as an indicator of organicity or a physiological etiology of unknown origin similar to how a clinical blood test is used as well as an objective evaluation of treatment efficacy upon follow-up. In the 1960s and 1970s, prior to the advent of MRI or PET scans or modern knowledge of brain function, it was speculated that the development of large qEEG databases of patients with different clinical disorders will result in the development of qEEG diagnostic measures that provide indications of psychiatric disorders [3]. However, it was quickly shown that only a statistical approach is feasible due to the number of measures and the fact that the EEG changes with age. As a consequence, age regression and stratified reference normative databases were developed by Matousek and Petersen in 1973 [4,5] and later by John [3,6–8], Duffy [9], Thatcher [10] and Congedo and Lubar [11], among others [12–17]. The Stockholm, Sweden, norms of Matousek and Petersen were independently replicated by John and collaborators in New York, USA [3,6]. Subsequent replications of different qEEG normative databases demonstrated the statistical stability and value of using reference normative databases to aid in identifying deviant EEG features and in linking the location of deviant features to symptoms and complaints [2–8,12,16,18]. The reference database provides a statistical match to reliable quantitative features available in the 1970s and 1980s. However, the spectral methods in the 1970s relied upon the Fourier transform that did not have sufficient temporal resolution to measure high-speed dynamics such as rapid shifts in phase differences and phase lock. This problem was solved in the late 1980s with the application of joint time–frequency analysis (JTFA), where a time series of real-time measures of phase differences is produced. JTFA provided precise measures of phase shift and lock durations across the human lifespan for all combinations of the ten- or 20-electrode systems and normative JTFA databases that were soon developed [12,19].

Efforts are still being undertaken in a few laboratories to record and classify qEEG from thousands of patients with the belief that a standalone diagnosis can be developed for different psychiatric disorders. However, as explained by John [2,3] and Duffy [9], it is unlikely that qEEG can serve as a standalone diagnostic measure no matter how large the databases. For example, meta-analyses of evidenced-based medicine criteria only show moderate to strong effect sizes for particular EEG features in schizophrenia [4] and obsessive–compulsive disorder, post-traumatic stress disorder, panic disorder, generalized anxiety disorder and phobias [2,20–22]. This scientific literature shows that there are a wide variety of different changes

in the amplitude and frequency of the EEG at the scalp surface, and effect sizes are too small to allow qEEG that is limited to the scalp surface to serve as a standalone diagnostic test, and this is why qEEG is best used as one test along with other clinical measures to aid a clinician to derive a diagnosis. In other words, evidenced-based medicine studies and other meta-analyses of 40 years of qEEG publications indicate that reliance solely on the surface qEEG is unlikely of providing a standalone diagnostic measure for a specific psychiatric disorder. In the realm of clinical science, this statement also holds true for the majority of clinical tests used by clinicians throughout the world; for example, blood test norms, bone density norms, sonograms, functional MRI (fMRI), PET and SPECT, among others, are rarely if ever used as a standalone diagnostic test.

In spite of the fact that the surface qEEG is not a standalone diagnostic test, recent advances in EEG tomography have nonetheless ushered in a new era for qEEG with increased value going beyond a general measure of 'organicity' to providing important information linking symptoms and complaints to functional systems in the brain and thereby enhancing qEEG's clinical value. It is these new advances in qEEG that are the subject of this article and the goal of this article is to note that in the decades to come, continued improvement and applications of EEG tomographic technology will change the face of neuropsychiatry by providing inexpensive clinical evaluation and treatment for psychiatric disorders. The reasons for this conclusion are twofold; one is because the spatial resolution of qEEG source analyses will be comparable with that of fMRI and PET scans but provide subsecond resolution that will be available at a fraction of the cost of other imaging methods; and the other is the fact that the brain is plastic and can be modified by biofeedback using 21st Century technology guided by the qEEG and the neuroscience of operant conditioning.

History of EEG tomography

'Tomography' means imaging by sections or sectioning. The word was derived from the Greek word 'tomos' which means 'part' or 'section' and represents the idea of a 'slice'. EEG tomography (tEEG; also known as qEEGt) is based on the ability to measure the location of 3D sources of the scalp surface EEG in the interior of the brain and then register the sources to MRI tomographic slices [23]. It is the coregistration of the

EEG sources to the MRI that is essential in the use of tEEG. Others refer to tEEG as 'electrical neuroimaging' [24] or 'brain electromagnetic tomography' (BET) [25]. The history of inverse methods is accurately described by Malmivuo and Plonsey, including the history of these methods in the field of cardiology in the 1800s [26]. In the 19th Century, Helmholtz mathematically proved that without constraints, the inverse problem has no unique solution. Subsequently, there is a long history of physiological constraints to aid in solving the inverse solution in physics and engineering using discrete and distributed source methods. Distributed source methods provide a smoother match to the tomographic MRI and are the dominant tEEG method in use today **(Table 1)**. Distributed methods often use the mathematical statistics of the minimum norm as a standard mathematical method in matrix algebra, discovered by Banach in 1922–1929 (e.g., L^p spaces and norms in the mathematics of linear functional analysis; i.e., Riesz's 1910 inverse solutions [27]). The minimum norm is special because it provides a unique solution to certain linear and nonlinear inverse solutions and has been applied to cardiology for decades before its application to EEG. For example, 1984 is the year that is most commonly attributed to the first application of a distributed linear solution to the electromagnetic sources of the EEG [28].

Efforts were made at NIH in the 1980s and in 1990–1994 to coregister all imaging modalities to a common anatomical atlas (i.e., the Talairach atlas and later the Montreal Neurological atlas), including EEG as part of the Human Brain Mapping project [23,29,30]. In the late 1980s, Michael Scherg developed discrete EEG/magnetoencephalogram (MEG) source solutions but only a distributed method such as those used in cardiology is acceptable for tEEG or BET [26,31,32]. In the late 1980s and early 1990s, many individuals worked on the application of distributed inverse solutions, and in 1992, Wang and collaborators were the first to apply the minium norm to the inverse problem of tEEG based on the mathematics of linear algebra and the science of electrical fields [33]. It was quickly found that a problem with the nonsmoothed minium norm is excessive weighting of sources near to the surface of the cortex. In 1994, Pascual-Marqui solved the problem of the surface bias by using a maximum smoothing constraint (spatial Laplacian) of the minimum norm [34]. The Laplacian operator pushed sources away from boundaries and regularized the matrix, resulting

Table 1. L^p classification of algebra distance metrics to solve inverse matrices.		
Norm	**Nonsmooth†**	**Smooth†**
L^0	Dipole [161] MUSIC [162,163]	–
L^1	Minimum current estimates [164]	VARETA [15] FOCUSS [165]
L^2	Minimum norm [28]	LORETA [34] LAURA [43] sLORETA [37] swLORETA [42]
Combination of L^1 and L^2	Combined minimum norm/minimum current [166]	Combined LORETA/VARETA [166]
Solutions of underdetermined linear equations involve minimization of vector distances. In mathematics, the L^p function spaces form an important class of topological vector spaces [27]. A norm is a function that assigns a positive length or distance to all vectors in a vector space and is used to find solutions to an underdetermined system of linear equations. †Smoothing is used to regularize underdetermined matrices in order to solve the linear matrix equations. Multiple fixed dipoles typically involve smoothing, while discrete dipole solutions do not involve smoothing. FOCUSS: Focal underdetermined system solution; L^0: Hamming norm; L^1: Taxicab norm; L^2: Euclidean norm; LAURA: Local autoregressive average; LORETA: Low-resolution electromagnetic tomography; MUSIC: Multiple-signal classification algorithm; sLORETA: Standardized low-resolution electromagnetic tomography; swLORETA: Standardized weighted low-resolution electromagnetic tomography; VARETA: Variable-resolution electromagnetic tomography. Data taken from [167].		

in unique solutions with sufficient spatial resolution to measure synchronous clusters of neurons in 7-mm^3 volumes of current sources, which is a fundamental property of the EEG. This method is called low-resolution electromagnetic tomography (LORETA) in which the term 'low resolution' does not mean low accuracy of the maximum current density voxel, but rather a smearing around the maximum current density [35]. The importance of statistical solutions of the inverse problem was introduced by Valdés in 1994 [36], resulting in a method called variable resolution electromagnetic tomography [15] and later a statistical normalization applied to LORETA called standardized LORETA [37]. The first tEEG normative databases using Z-scores and Gaussian distributions similar to what is used in fMRI [38] and referred to as 'statistical parametric mapping' was introduced by Valdés and coworkers in 2001 [15] followed by Thatcher and coworkers in 2005 [39,40].

Subcategories & validation of tEEG
Today, there are many different BET or tEEG methods using *a priori* assumptions imposed on the solutions. The two subcategories of inverse solution are described in **Table 1** [41]. The matrix norm and the two categories: nonsmooth and smooth include standardized weighted LORETA [42] as a standardized version of the depth-weighted minimum norm and local autoregressive average [43].

There are hundreds of accuracy validation studies in the scientific literature of tEEG showing spatial resolutions on the same order as fMRI and sufficiently accurate to measure Brodmann areas [44,45]. For example, for LORETA alone there are 795 publications listed on the internet in 2009 [202] and the National Library of Medicine cites 373 citations of LORETA in 2010 and 2011.

It is easy to demonstrate that different samples of EEG yield the same localization and/or that a particular local event in the EEG corresponds to an expected source of that event; for example, α-spindles are at a maximum in the occipital cortex Brodmann areas 17 and 18 by LORETA and are not somewhere unexpected, a right hemisphere hematoma is localized to the right parietal lobe or hemiretinal stimulations shift current sources based on the connections between the retina and cortex. These are examples of content validity. The reliability and validity of LORETA source localization has been further demonstrated using mathematical simulations, stimulating from implanted electrodes in epileptic patients and standard tests, as well as by determining that the distribution of current sources is represented by a Gaussian distribution [15,39–41].

The advent of tEEG is important because it provides for co-registration of an imaging modality to regions of the brain similar to those imaged by fMRI and PET that measure blood flow. tEEG is similar in spatial resolution to fMRI but adds high temporal resolution of the electrical sources in the brain that give rise to changes in blood flow. tEEG also provides for 3D network analysis including source coherence and phase differences and source phase reset at high temporal resolutions using JTFA.

The spatial cross-validation studies of distributed inverse solutions such as LORETA/variable-resolution electromagnetic tomography and other inverse solutions are both mathematical and empirical. Pascual-Marqui and coworkers [34,35] provide mathematical cross-validation accuracies for LORETA, standardized LORETA and exact LORETA. Frequency and time mathematical cross-validation by Gomez and Thatcher demonstrated equivalence in the time and frequency domain, which is important when using JTFA [46]. Empirical cross-validation studies used simulations from implanted electrodes in epileptic patients, phantom head models, physiological experiments using different stimulus modalities and using diffusion-weighted spectroscopy of connection density and cross-validation in traumatic brain injury, stroke and tumor patients confirmed by MRI T_2 relaxation time [47–49,202]. Cross-validation studies of LORETA have also been published with respect to normative Z-scores in stroke patients, tumor patients and epileptic patients, as well as in combined fMRI and/or SPECT studies in depression, traumatic brain injury and other neuropsychiatric disorders [202].

An important fact that will influence the future of neuropsychiatry is that tEEG provides a portable subsecond measure of 3D functional coupling between brain regions. With JTFA, computation times are in microseconds and time resolution is the sampling rate, whereas 1–8 ms resolutions at 128–1000 Hz are common in the science of qEEG. This includes phenomena that are invisible to the human eye such as subsecond animation of Brodmann area phase shift and phase lock, which is known to be fundamental to brain function [1,19]. Psychiatrists, neuropsychologists and neurologists are currently using these methods to link patients' symptoms and complaints to functional systems in the brain to implement treatment via brain–computer interfaces (BCI) and neurofeedback (NF) technology. The following paragraphs are a brief review of modern knowledge about the EEG and some of the growing applications of high-speed computers and biofeedback to improve mental health.

The large expansion of knowledge about the functions of the brain prompted by the 'decade of the brain' in the 1990s and continuing into the 21st Century is now prompting a widespread use of qEEG for clinical evaluation, treatment decisions and monitoring treatment efficacy. For example, the last 40 years of neuroscience have shown that specialized groups of neurons mediate specific functions that operate in parallel and are integrated into large dynamic systems that are briefly phased locked in an integrated and coordinated manner to mediate adaptive functions [1,19,50–62].

Neurological and neuropsychological studies have shown that integrated function is global and not located in any one part of the brain [63,64]. Instead the brain is made up of complex and interconnected groupings of neurons that constitute 'functional systems', such as the 'digestive system' or the 'respiratory system', in which cooperative sequencing and interactions give rise to an overall function at each moment of time [63]. This widely accepted view of brain function became dominant in the 1960s and 1970s and is still the accepted view today. For example, since the 1980s, new technologies such as fMRI, PET, SPECT and qEEG/MEG have provided numerous examples of psychiatric symptoms linked to instabilities and deregulation of specialized brain systems [13,29,30].

Modern PET, qEEG, MEG and fMRI studies are consistent with the historical view of coordinated 'functional subsystems' and show that the brain is organized by a relatively small subset of 'modules' and 'hubs' that represent clusters of neurons with high within-cluster connectivity and sparse long-distance connectivity [65–68]. Modular organization is a common property of complex systems and 'small-world' models fit best because maximum efficiency is achieved when local clusters of neurons rely on a small set of long-distance connections in order to minimize the 'expense' of communication. This is an explanation of why long-distance connections appear to be vulnerable to aging in general and why the loss of distant connections is a predictor of early stages of Alzheimer's disorder [69–72].

Normative qEEG databases

The first normative qEEG reference databases were developed in the 1960s through to the 1980s, providing comparisons of individuals with groups of age-matched healthy individuals. These databases are used clinically in a similar way that blood analyses are used to compare an individual with a group of healthy individuals [2]. During the 1990s and 2000s normative qEEG databases were extended to 3D source localization registered to the Talairach atlas [15,34,35,40,41]. These databases provide a simple and easy-to-use statistical Z-score as a metric by which estimates of the

location and extent of deregulation with respect to a group of age-matched and healthy individuals can be measured offline or in real-time. Electrical neuroimaging normative databases of Brodmann areas and hubs and modules when linked to the patient's symptoms and complaints aids a clinician, along with other measures to derive a diagnosis. In addition, normative qEEG database Z-scores help evaluate the course of treatment such as medications, repetitive transcranial magnetic stimulation (rTMS) or biofeedback and thereby help evaluate the comparative efficacy of treatment [2–15,36,40,41].

Normative reference databases spanning the age from birth to senescence are used to compare a patient's EEG current sources to an age-matched group of normal subjects [2–15,39–41]. Another confirmation of the content and construct validity of a normative LORETA database involves testing the accuracy of a normative database using patients with confirmed pathologies where the location of the pathology is known by other imaging methods (e.g., CT scan, MRI or PET). Validity is estimated by the extent that there is a high correspondence between the location of the confirmed pathology and the location of the 3D sources of the EEG that correspond to the location of the pathology. The following is a partial list of studies showing concordance validity with fMRI and LORETA [17,73–79], between PET and LORETA [80–83] and between SPECT and LORETA [84].

'Coherence' is a measure of coupling between groups of neurons and 'phase differences' are a measure of time delays due to conduction velocity, synaptic delays and synaptic rise times in neural networks. 'Hypercoherence' is related to reduced functional differentiation and 'hypo-coherence' is related to reduced functional connectivity [2,3,7,8,10]. Phase shift and phase lock duration are correlated with coherence and are measured in milliseconds and reflect fundamental processes involved in the coordination of neural activity located in spatially distributed 'modules' at each moment of time and at all levels of the nervous system [1,19,52–62]. Importantly, only EEG/MEG has sufficient spatial and temporal resolution to measure the millisecond dynamics of modules and hubs and use Z-scores to estimate deregulation in brain regions that can be linked to the patient's symptoms and complaints. In comparison with MEG, qEEG can better detect deeper cortical sources and is not limited to only tangential dipoles. In addition, MEG is expensive, being in the order of hundreds of thousands of

US dollars and with high monthly maintenance costs whereas qEEG is less than US$10,000, there are no monthly maintenance costs and it is portable. The use of modern qEEG methods provides accurate evaluation of deregulated brain regions linked to symptoms in the anatomical, PET, fMRI and EEG/MEG literature and can lead to better treatment decisions and improved monitoring of the efficacy of treatment (this knowledge is so widespread that today, Google searches of symptoms and brain systems provide the anatomical linkages).

The clinical treatment aspect of qEEG is represented by the science of BCIs and EEG biofeedback, also called NF. EEG BCI and NF clinical treatment is based on the use of reinforcement and operant conditioning to train patients to modify specific EEG frequencies and phases at particular scalp locations, including the use of 3D source analysis to modify the EEG generated in specific brain regions such as the anterior cingulate gyrus or lateral prefrontal lobes, among others [85–92]. Operant conditioning of specific brain regions has also been used with fMRI, but this method is very expensive with low temporal resolution and long delays between brain changes and reinforcement [93]. Another clinical treatment is the application of magnetic pulses referred to as rTMS that momentarily disrupts the ongoing electrical network dynamics, acting like a perturbation after which the cortex converges to a new stable state [94,95]. Even low levels of magnetic pulses can affect the phase coupling in the EEG and similarly can temporarily disrupt the normal and ongoing activity followed by a new and different stable state. Combining qEEG and rTMS allows clinicians to refine the duration and location of magnetic stimulation and more accurately target deregulated brain regions linked to the patient's symptoms and complaints. Clinical qEEG treatment can include a two-stage procedure of rTMS that briefly resets neural dynamics followed by EEG biofeedback to train the brain dynamics towards the mean of a reference group of age-matched normal subjects.

Clinical applications of electrical neuroimaging

Figure 1 provides a comparative perspective of the temporal and spatial resolution of different neuroimaging modalities. As discussed later, electrical neuroimaging using the discrete inverse solution has a maximum spatial resolution of approximately 1 cm^3 with one or two dipoles

and the highly accurate multidipole method called LORETA has maximum resolutions of approximately 1–3 cm.

Deregulation of specialized parts of an integrated system can be identified as well as compensatory processes, thereby providing a more comprehensive understanding of the patient's symptoms and complaints and also aiding in the evaluation of treatment. Some are hesitant to use qEEG for the purposes of electrical neuroimaging in the same manner as fMRI or PET is used because of the mistaken belief that qEEG has low spatial resolution. However, as reviewed in later sections, there are more than 700 peer reviewed publications [202] that use the same voxel sizes for EEG distributed inverse solutions at 7 mm^3 and with spatial resolutions of approximately 1–3 cm^3 [15,34,35]. By contrast, the best spatial resolution of fMRI is approximately 4 mm^3 under the most ideal circumstances, but is often several centimeters, which is a similar spatial resolution as tEEG [90,91]. The advantage of electrical neuroimaging over fMRI and PET is the reduced cost and the marked improvement in temporal resolution. Comparative studies of the respective spatial resolutions of qEEG and MEG show that although the high resistivity of the skull decreases the spatial resolution of qEEG, it does not make it worse than that of MEG. In fact, if special care is taken to address the considerable influence of the shape and conductivity of the volume conductor, the localization accuracy of qEEG could be equivalent or even superior to that of MEG [96–98].

Spatial & temporal scaling

Neurons rapidly synchronize and the spatial extent of global or macroscopic function is approximately 1–6 cm if fMRI or PET or any other imaging modality is used. This indicates that synchronization of large groups of pyramidal neurons is itself a fundamental property of information processing in the human brain. Another important fact is that the axonal connections of the human cortex are arranged in six basic clusters referred to as 'modules', as measured by diffusion-imaging spectroscopy [65]. The synaptic density of connections is spatially heterogeneous and clustered with phase shift and phase lock between clusters or modules, providing the 'vitality' or temporal dynamics of the qEEG as mediated by stable loops in
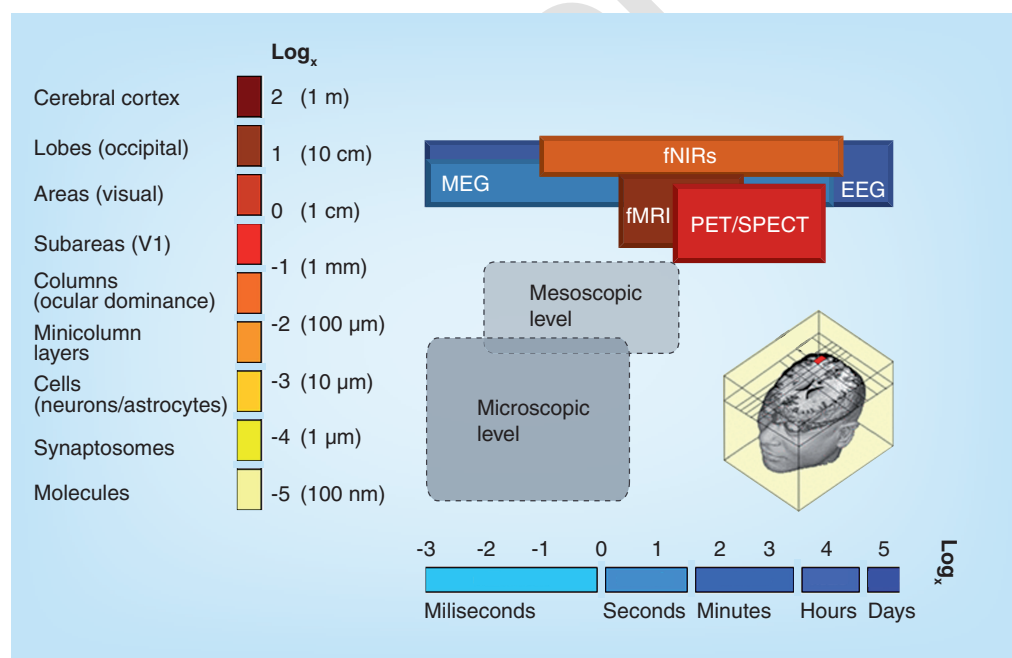

Figure 1. Comparative spatial and temporal resolutions of different neuroimaging methods. The y-axis is the log$_{10}$ of space and the x-axis is the log$_{10}$ of time. The nested dynamics of the microscopic and mesoscopic levels within the macroscopic level is illustrated. Quantitative EEG spatial resolution ranges from approximately 7 mm^3 to 6 cm^3 and temporal resolution is less than 1 ms, with the ability to measure events over a 24-h period of time.
fMRI: Functional MRI; fNIR: Functional near infrared; MEG: Magnetoencephalogram.

thalamo–cortical, cortico–thalamic and cortico–cortical connections. Pacemakers and the natural resonance of pyramidal neurons and loops give rise to stable rhythms that operate like a 'carrier wave' in which phase shift of neurons with respect to the local field potential to 'in-phase', where they are excited, to 'anti-phase', where they are suppressed, is orchestrated by phase shift and phase lock mechanisms that are easily measurable in real-time by standard qEEG methods [1,99–105].

Figure 2 illustrates the relationship between the micro-, meso- and macro-scopic levels of spatial and temporal scaling and emphasizes the role of phase shift and phase lock as basic causal mechanisms that link all levels and are reflected in the qEEG, especially with respect to functional modules in the brain.

Quantitative EEG measures such as directed short- and long-distance coherence, phase delays, phase locking and phase shifting of different frequencies at millisecond time resolutions are essential in understanding how specialized neurons at the microscopic, mesoscopic and macroscopic levels are spatially and temporally scaled with lower frequencies (e.g., δ: 0–4 Hz; and τ: 4–8 Hz) and phase synchronized to higher frequencies (e.g., α: 8–12 Hz; β: 12–20 Hz; and γ: 20–50 Hz) [1,15,47,106–111]. The qEEG reflects top-down causality at the macroscopic level by coordinating the meso- and micro-scopic levels of neural organization by scaled temporal and spatial frequencies and time constants. It is the low spatial and temporal frequencies of the macroscopic level that are the order parameters to coordinate and synchronize the micro- and meso-scopic levels, and this is another reason why the macrodynamic EEG is so important in clinical evaluation and treatment. The deregulation of specialized groups of neurons at micro- and meso-scopic levels that simultaneously mediates specialized functions can be measured at the macroscopic level using qEEG.

qEEG & phase lock & phase shift of neural modules

The rapid creation and destruction of multistable spatial–temporal patterns have been evaluated in evoked, transient and spontaneous qEEG studies [112–114]. As described earlier, modern neuroscience shows that the patterns of spontaneously occurring synchronous activity involve the creation of differentiated and coherent neural assemblies at micro-, meso- and macro-scopic scales. The dynamic balance between synchronization and desynchronization is essential for normal brain function, and abnormal balance is often associated with pathological conditions such as epilepsy [70,115–117], dementia [118,119], traumatic brain injury [120], cognitive function [121–125], working memory [126,127], sensory–motor interactions [128,129], hippocampal long-term potentiation [130], intelligence [52], autism [62] and consciousness [131–135].

Phase shift and phase lock can also be measured in real-time, which means that these measures can be used for BCI and qEEG biofeedback (i.e., NF) purposes, as discussed in a later section. **Figure 3** provides an example of the effect size and fundamental importance of phase reset in a study of autism. One of the advantages of phase shift and lock duration is that they are measured in the time domain and are correlated with inhibitory postsynaptic potential and excitatory postsynaptic potential synaptic durations [100–104]. **Figure 3A & 3B** are histograms
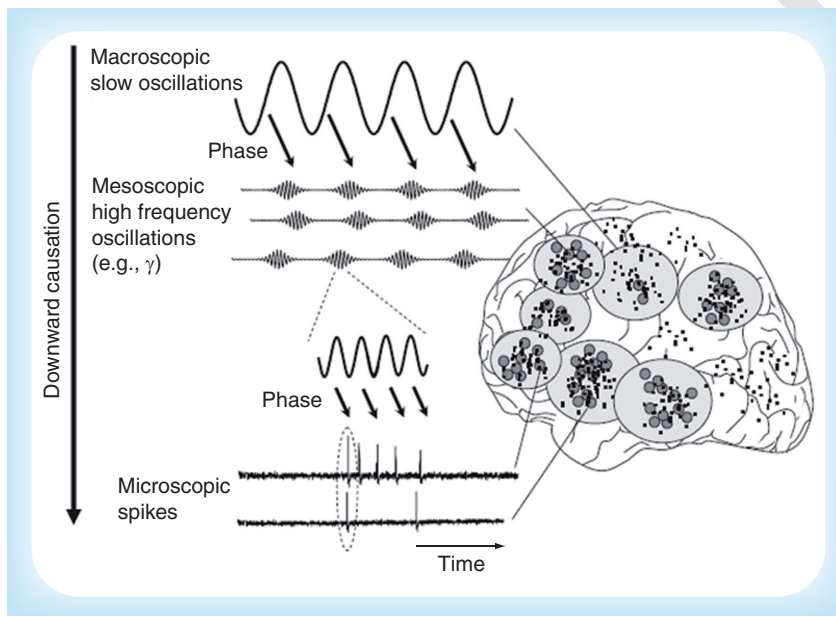

Figure 2. Multifrequency oscillations for scaling up or down in brain dynamics.
The macro-, meso- and micro-scopic processes are braided together by co-occurring oscillations at successively faster frequencies that modulate each other by variations of the underlying neuronal excitability. In particular, through their phases, global brain oscillations in the low-frequency range (<4 Hz) may constrain local oscillations in the high-frequency range (40–200 Hz; e.g., γ-oscillations). In turn, these high-frequency oscillations determine, in the millisecond range, the probability of occurrence of spikes and of their temporal coincidences between different brain regions.
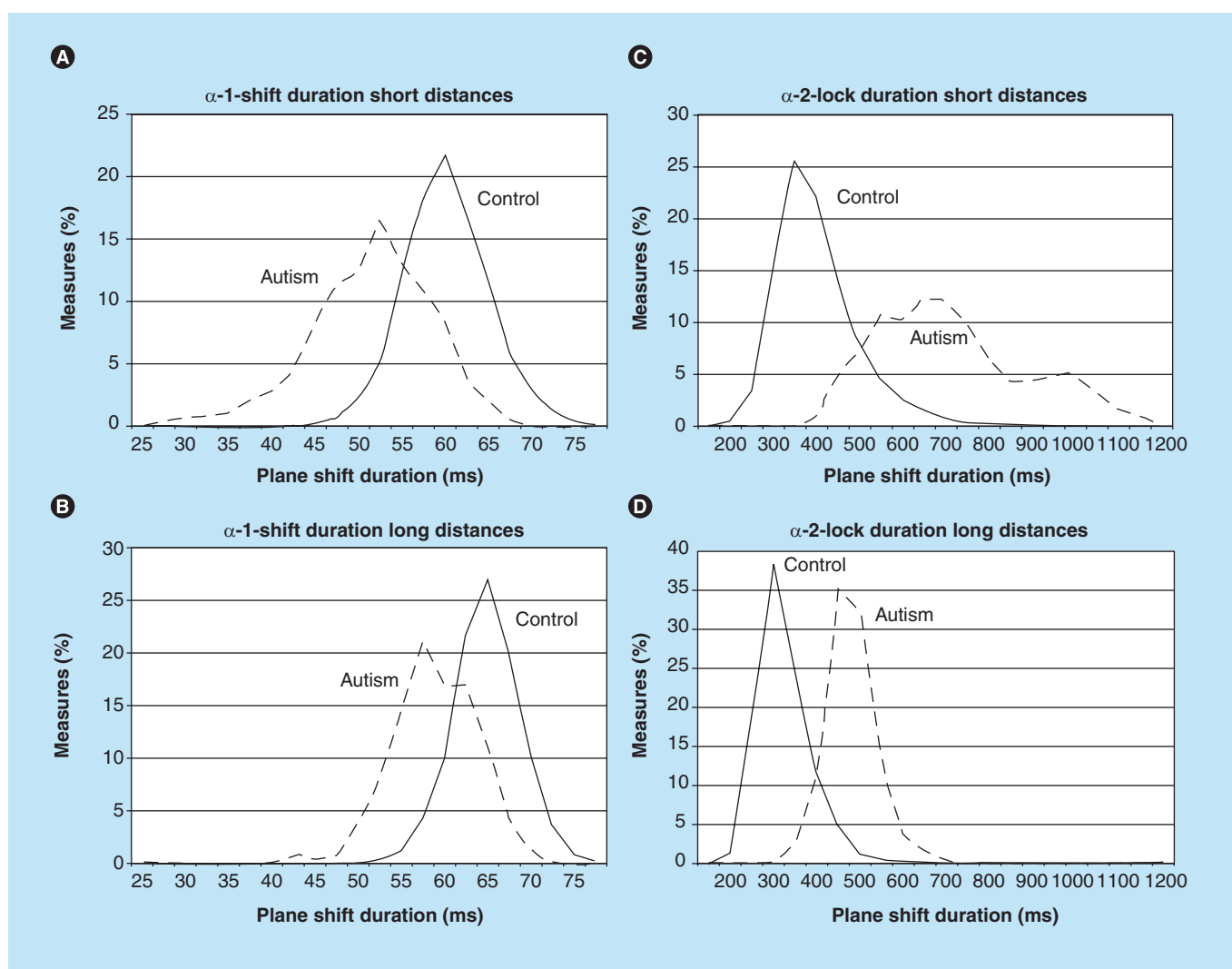Reproduced with permission from [168].

Figure 3. Histograms of the percentage of phase shift and phase lock duration measures in control and autistic subjects. The y-axis is the percentage of measures and the x-axis is phase shift duration (ms) in the α-1 (8–10 Hz) frequency band in **(A)** and **(B)** and phase lock duration (ms) in the α-2 (10–12 Hz) frequency band on the right in **(C)** and **(D)**. **(A & C)** Histograms for short interelectrode distances (6 cm). **(B & D)** Histograms for long interelectrode distances (21–24 cm) in control (solid lines) and autistic subjects (dashed lines) [85].

of phase shift durations of short and long inter-electrode distances in the α-1 frequency band (8–10 Hz) in a group of autistic spectrum disorder children (dashed lines) and an age-matched control group (solid lines). **Figure 3C & 3D** are histograms of phase lock durations of short and long interelectrode distances in the α-2 frequency band (10–12 Hz) in autistic versus control subjects. This figure shows that phase shift duration is shorter in autistic subjects than control subjects in the α-1 frequency band (8–10 Hz) and that phase lock duration is longer in autistic subjects in the α-2 frequency band (10–12 Hz) independent of interelectrode distance [62].

tEEG & diffusion spectral imaging 'modules'

As mentioned earlier, convergent evidence from different imaging modalities has demonstrated that the human brain is a network organized by 'nodes' with linkages and clustering of connections defined as 'modules' based on the density of synaptic connections and constituting 'functional modules' [136]. Graph theory is commonly used to quantify the structural topology of the human brain using different imaging methods and achieving similar results from diffusion spectral imaging (DSI), fMRI and qEEG/MEG [65,80–82,119,137,138]. Recently, Hagmann and coworkers used DSI and tractography to trace the

cortical white matter connections of the human cerebral cortex between 66 cortical regions with clear anatomical landmarks [65], using the same gyri and sulci as used by von Brodmann [139] and is still used in all of the neuroimaging technologies today. Network spectral analyses of nodes and edges of the regions of interest were grouped into six anatomical modules with maximum centrality defined as high within-density anatomical connectivity [65]. The six main anatomical connection density modules include, but are not exclusively, the posterior cingulate, the bilateral precuneus, the bilateral paracentral lobule, the unilateral cuneus, the bilateral isthmus of the cingulate gyrus and the bilateral superior temporal sulcus.

Quantitative EEG using electrical neuroimaging methods such as LORETA shares the ability to link synchronous neural activity registered to a common and standardized anatomical Talairach atlas [23,140,141], as well as to an age-matched normative database with Z-scores in real-time. Because local synchrony of neurons is necessary to produce a recordable scalp EEG, another constraint is that the density of synapses in clusters of pyramidal neurons is positively related to current source density in a given volume of the brain. Spatial correlation of LORETA spectral amplitudes is a measure of the spatial–temporal synchrony of neurons located in different regions of interest and in different Brodmann areas [113,114,128,139,142,143].

Several studies have used electrical neuroimaging coherence and correlation to investigate electrical coupling in different Brodmann areas [68,141,144–146]. Lehman and coworkers computed coherence and phase lock between regions of interest in resting versus meditating subjects [147]. Thatcher and coworkers used LORETA spatial correlations and demonstrated spatial undulations and regular spacing of correlations as a function of distance [148]. All of these qEEG studies revealed interesting and reproducible relations between current sources and network connectivity that are independent of volume conduction and provide a deeper understanding of surface EEG dynamics. For example, in the Thatcher and coworkers study, regions that had the highest neuron packing density exhibited the highest nearest neighbor source correlations [148] and a model of a 'U'-shaped cortico–cortical fiber system fits the spatial patters of source correlations **(Figure 4)** [149,150].

Given the large scientific literature in support of accurate qEEG source localization, it is reasonable to hypothesize that there is a linkage between structural MRI and LORETA because diffusion weighted images reflect anatomical connectivity (axons) and anatomical connectivity is the basis for effective connectivity (one region influencing another); therefore, it follows that the MRI should predict synchrony between distant brain regions as measured by LORETA and all distributed inverse solutions. Thatcher and coworkers tested the null-hypothesis that LORETA current sources exhibit a random clustering and random ranking of correlations [146] that are not like the anatomical clusters or modules measured by DSI in the Hagmann and coworkers study [65]. This hypothesis was rejected because the results demonstrated statistically significant spatial correspondence between EEG source analysis and the anatomical density of connectivity as measured by MRI. The spatial 'clustering' of qEEG source correlations were not random and instead were the same as observed with MRI. A simple explanation of why qEEG source correlations are spatially 'clustered' in the same manner as MRI is because synaptic densities are measured by both MRI and EEG source analyses. qEEG differs from MRI by higher temporal resolution of phase shift and phase lock or synchrony between time series of sources; however, the six basic anatomical 'clusters' are present in the two different measurement domains, thereby demonstrating a linkage between structural MRI and dynamical EEG. This is important because it provides another cross-modality validation of electrical neuroimaging as a neurophysiologically useful measure of the preconscious and conscious mind. The Hagmann and coworkers 'modules' are also functional modules in that each involves different specialized brain regions clustered in functional groups [65]. Coregistration of qEEG sources to the Hagmann and coworkers anatomical clusters allows for a spatial reference by which phase dynamics and fine temporal coherence within and between 'modules' can be analyzed [65].

Figure 5 shows an example from Thatcher and coworkers [146] of the replication of the Hagmann and coworkers DSI modules using qEEG [65].

qEEG & cortico–cortical connections

Volume conduction occurs because synchronous electrical sources produce an electrical field with zero phase lag that falls off smoothly and rapidly with distance. It is also known that the greater the connectivity between neurons then the higher the amplitude of qEEG because connectivity is necessary for synchrony. Anatomical studies also demonstrate a smooth
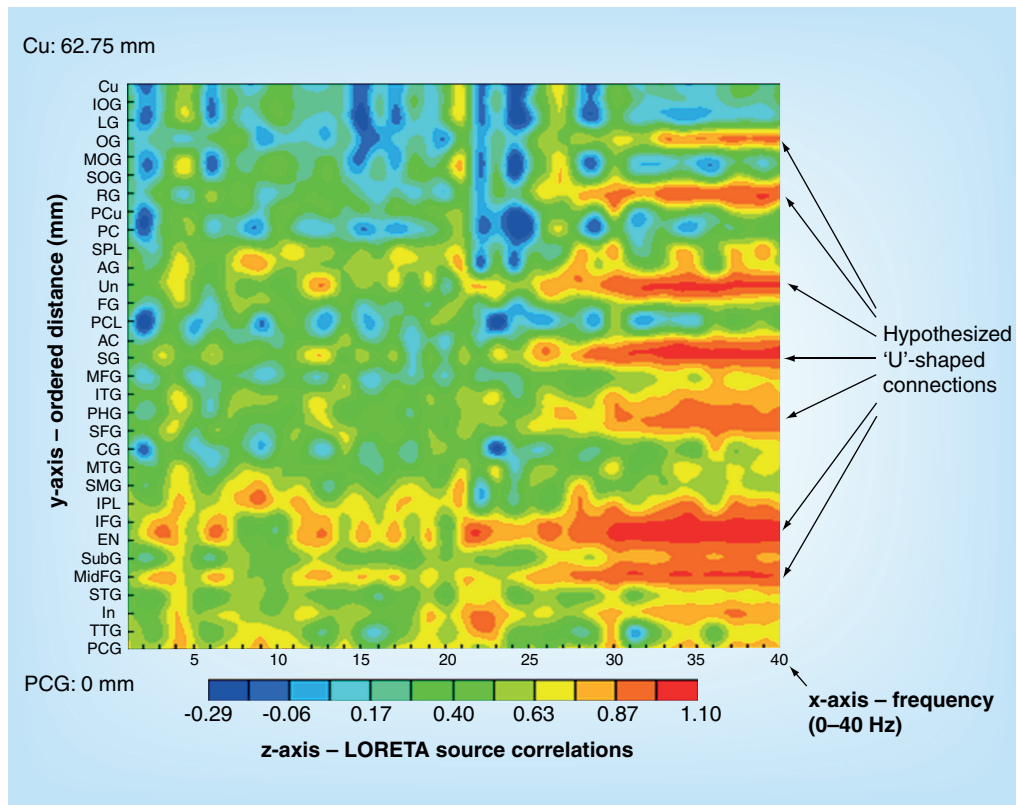
Figure 4. An example of one of the subjects demonstrating spatial heterogeneity of low-resolution electromagnetic tomography source correlations that cannot be explained by volume conduction. The regions of interest are ordered as a function of distance from the reference Brodmann area 1 or left postcentral gyrus to the left cuneus (Brodmann area 17, which is 62.75 mm distant). The x-axis is frequency (1–40 Hz), the y-axis is regions of interest and the regions of interest are ordered as a function of distance from the postcentral gyrus. The z-axis is the magnitude of the LORETA source correlation as represented by the color bar of the contour map. The blue to red line represents a regular spacing of increases and decreases in coupling with a spacing consistent with the 'U'-shaped fiber system of the human cortex. The 'U'-shaped fibers are strongly coupled at 20–40 Hz. The alternating vertical red and blue represent a regular spacing of frequency in which a specific Brodmann area is coupled with many other Brodmann areas but only within a particular frequency band (e.g., τ and β and α and γ). The cortico–cortical fiber system is highly coupled at 20–40 Hz and less coupled in the lower frequency ranges.
AC: Anterior cingulate; AG: Angular gyrus; CG: Cingulate gyrus; Cu: Cuneus; EN: Extranuclear frontal gyrus; FG: Fusiform gyrus; IFG: Inferior frontal gyrus; In: Insula; IOG: Inferior occipital gyrus; IPL: Inferior parietal lobule; ITG: Inferior temporal gyrus; LG: Lingual gyrus; LORETA: Low-resolution electromagnetic tomography; Mid dFG: Middle frontal gyrus; MFG: Medial frontal gyrus; MOG: Middle occipital gyrus; MTG: Middle temporal gyrus; OG: Orbital gyrus; PC: Posterior cingulate; PCA: Posterior central gyrus; PCG: Postcentral gyrus; PCL: Paracentral lobule; PCu: Precuneus; PHG: Parahippocampal gyrus; RG: Rectal gyrus; SFG: Superior frontal gyrus; SG: Subcallosal gyrus; SMG: Supramarginal gyrus; SOG: Superior occipital gyrus; STG: Superior temporal gyrus; SubG: Subgyral region; TTG: Transverse temporal gyrus; Un: Uncus.
Reproduced with permission from [146].

decrease in synaptic density as a function of distance from any collection of neurons [149–152]. Thus, electrical volume conduction and connection density are confounded to some extent, especially in the short-distance domain. Schulz and Braitenberg showed that there are three categories of cortico–cortical connections in the human brain: intracortical connections that
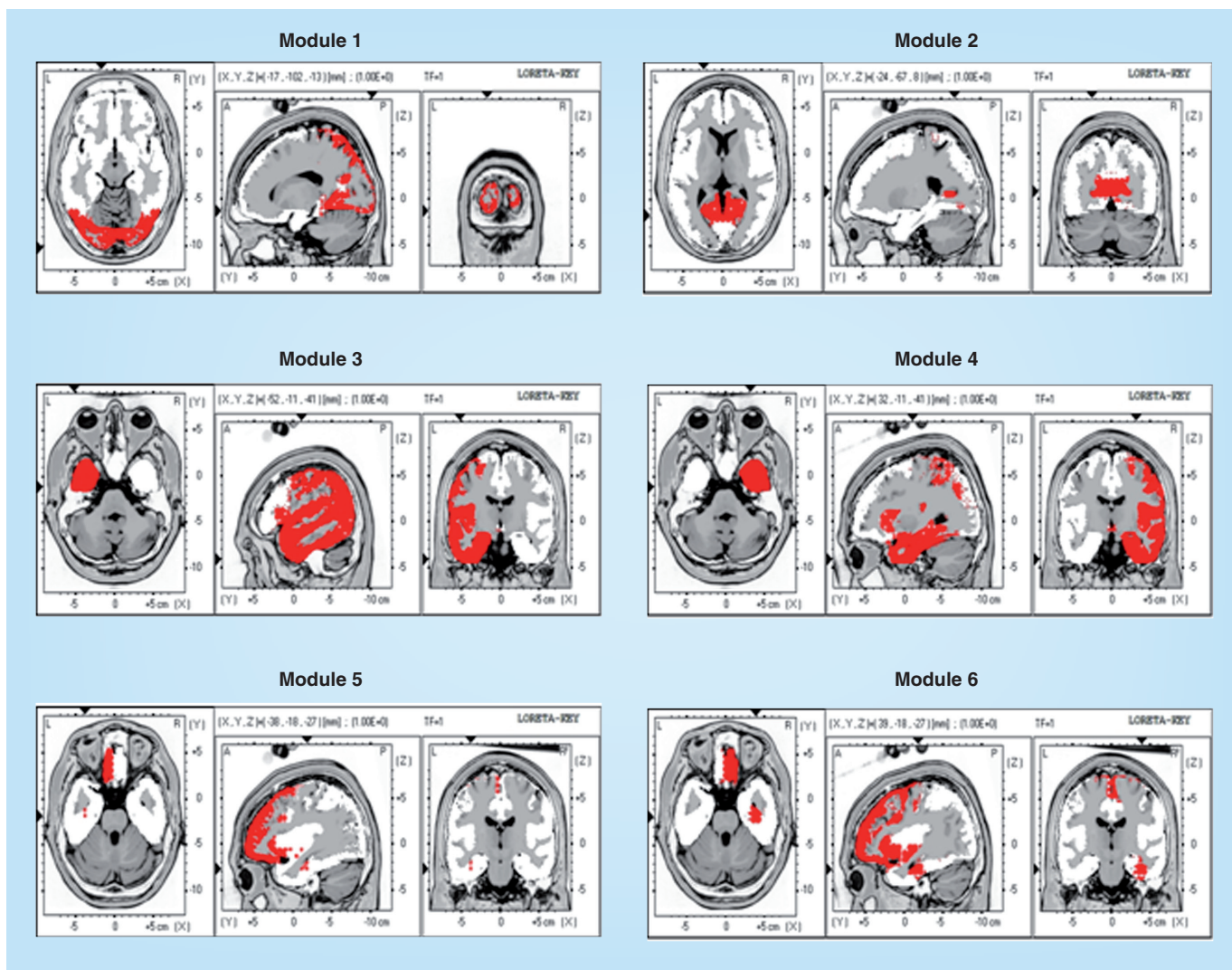
Figure 5. Spatial heterogeneity of EEG source correlations. The locations of the six Hagmann *et al.* modules [65] as represented by the key institute low-resolution electromagnetic tomography voxels (Lancaster *et al.* [23]). As per Hagmann *et al.* [65], modules 3 and 4 are the same but from different hemispheres.
Reproduced with permission from [146].

represent the majority of cortical connections and are on the order of 1 mm to approximately 5 mm and involve collateral axonal connections that do not enter the cerebral white matter; 'U'-shaped myelinated fibers representing the majority of the cerebral white matter that connects cortical gyri and sulci and are on the order of 3 mm–3 cm; and deeply located long-distance fiber systems referred to as fasciculi with connections from approximately 3 to 15 cm that represent approximately 4% of the cerebral white matter [153]. The intracortical fiber system is too short at 1–3 mm for 19-lead or even 512-lead EEG to resolve connectivity differences at the scalp surface [87]. Nonetheless,

the effects of the intracortical system on the amplitude of the EEG are strong because fiber bundles carry action potentials that produce somadendritic excitatory postsynaptic potentials and thereby synchronize large groups of neurons [154,155].

Low-resolution electromagnetic tomography source correlation studies have demonstrated spatial heterogeneity that is consistent with the studies by Schulz and Braitenberg [153], especially in the longer distances, and these studies cannot be explained by volume conduction. **Figure 4** is an example of increases and decreases in source correlations as a function of distance in a subject in this study with a pattern consistent with the

Schulz and Braitenberg cortico–cortical connection model that cannot be explained by volume conduction [153].

Z-score biofeedback

Operant conditioning of specific EEG frequencies has been published in over 690 EEG biofeedback studies since the 1960s (search the National Library of Medicine with the search terms 'EEG biofeedback' for a listing of studies) and 2348 BCI studies. Evidence-based medicine designs and meta-analyses show the relative efficacy of EEG biofeedback [156,157]. Often more than 40 sessions of EEG biofeedback are required to achieve improved clinical outcome. Although it is beyond the scope of this article to review the EEG biofeedback literature, it suffices to say that the goal of future clinical applications of EEG biofeedback is to obtain better clinical outcomes in fewer sessions. One approach to achieve improved clinical outcomes in fewer sessions is to target the 'weak' systems of the brain that are linked to the patient's symptoms and to avoid modifying compensatory networks. A recent method to improve the clinical efficacy of EEG biofeedback is the use of real-time age matched normative database comparisons to scalp locations and Brodmann areas using Z-scores. The Z-scores or standard deviations with respect to an age-matched reference population provide a real-time guide to train patients toward Z = 0 in brain regions associated with particular disorders [158–160]. The clinical use of qEEG in neuropsychiatry involves three distinct steps: a clinical interview and evaluation of the patient's symptoms and complaints; linking the patient's symptoms to functional specializations in the brain based on the scientific literature (qEEG/MEG, fMRI, PET and SPECT, among others); and real-time Z-score biofeedback to modify deviant or deregulated brain regions associated with the patient's symptoms and complaints.

Figure 6 is an example of various functions associated with particular Brodmann areas based on fMRI, PET, EEG/MEG and lesion/tumor studies [63,64]. Convergence of classical and well-established studies that link clinical disorders to functional specialization helps clinicians to target variables for EEG biofeedback, and the use of real-time Z-scores aids in reinforcing regulation of unstable brain systems linked to the patient's symptoms. **Figure 7** shows an example of LORETA Z-score biofeedback selections using a symptom checklist and/or a neuropsychological assessment checklist to target deregulated brain regions and reinforce EEG variables towards Z = 0, which is the center of the healthy normative database values.

Clinical practice points

The application of qEEG to determine 'organicity', to link to symptoms and to evaluate treatment efficacy has been its mainstay for the last 40 years. Treatment using qEEG biofeedback is growing and is being applied in clinics throughout the world. The practical steps involved in the clinical application of qEEG for both assessment of organicity and biofeedback include:

- Measure eyes open and eyes closed artifact free qEEG;
- Use auto- and cross-spectra to identify scalp locations and network deviations from normal;
- Use tEEG to identify deregulation in brain systems linked to the patient's symptoms and complaints;
- Separate the 'weak' systems from the possible compensatory systems;
- Use the qEEG to decide treatment modalities and then follow-up evaluations to determine treatment efficacy (medications, rTMS, electroconvulsive therapy, BCI and biofeedback, among others);
- If surface qEEG and tomographic Z-score biofeedback is used, then target the deregulated brain subsystems to reinforce optimal and homeostatic states of function while the clinician monitors the patient's symptom reduction. Use the patient's feedback to change protocols.

A growing number of clinicians are adding qEEG assessment to link a patient's symptoms and complaints to deregulation of functional systems in the brain followed by one or more treatments followed by follow-up evaluation to assess treatment efficacy.

Conclusion & future perspective

Reliance solely on surface EEG patterns without linking a patient's symptoms and complaints to locations and systems in the brain has resulted in only moderate clinical utility of the qEEG. A new era of tEEG has arisen that is inexpensive and portable and that will affect the convergence

of neurology, neuropsychology and neuropsychiatry in the decades to come. The ability to link a patient's symptoms and complaints to functional specializations in the brain is essential to understanding a patient's disorder. The location of deregulated brain regions is most important because it provides a link to two centuries of neurology and other neuroimaging methods such as PET, fMRI, SPECT, as well as structure determination by MRI and diffusion tensor imaging, with the advantage of millisecond time resolution. In the 21st Century, the Talairach atlas coordinates linked to the patient's symptoms provide a type of cross-validation so that the clinician can use a simple Google search or search of the National Library of Medicine of the scientific
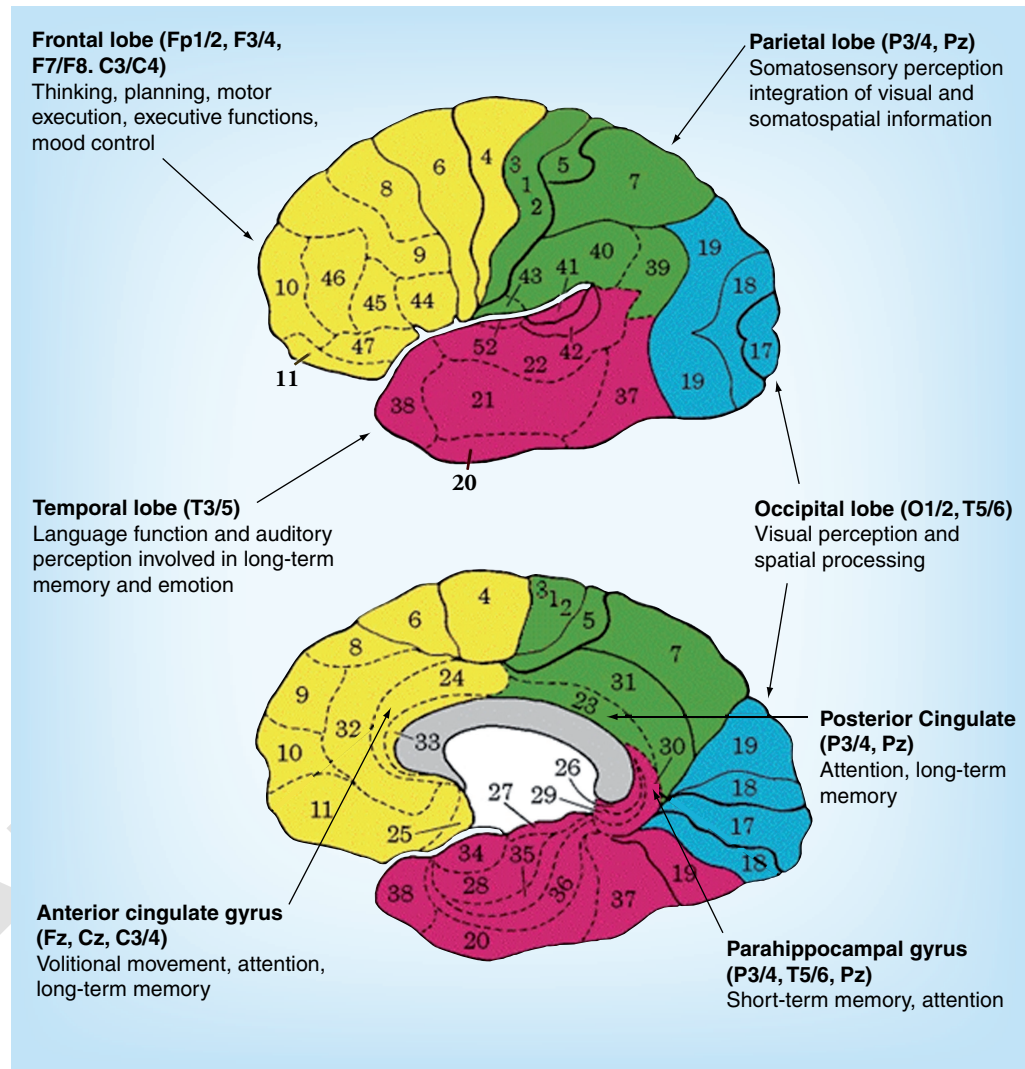

Figure 6. Illustration of Brodmann areas linked to particular functions. Brodmann areas operate at the macroscopic level as measured by the quantitative EEG with spatial areas of common functional cytoarchitecture that range in size from approximately 1 to 6 cm³. The goal is to link a patient's symptoms and complaints to deregulation or deviation from normal in brain regions known to be related to specific functions. Quantitative EEG also provides high temporal resolution so that measures of dynamic connectivity and phase reset can also be evaluated with respect to an age-matched normative database. Treatment follows assessment in order to 'move' deregulated subsystems and global linkages towards the normal range of function. This approach is similar to the use of a blood test to identify deviant constituents of the blood (e.g., elevated liver enzymes or white blood cell count) that can be linked to the patient's symptoms and aid in the decision for treatment and in monitoring the efficacy of treatment.
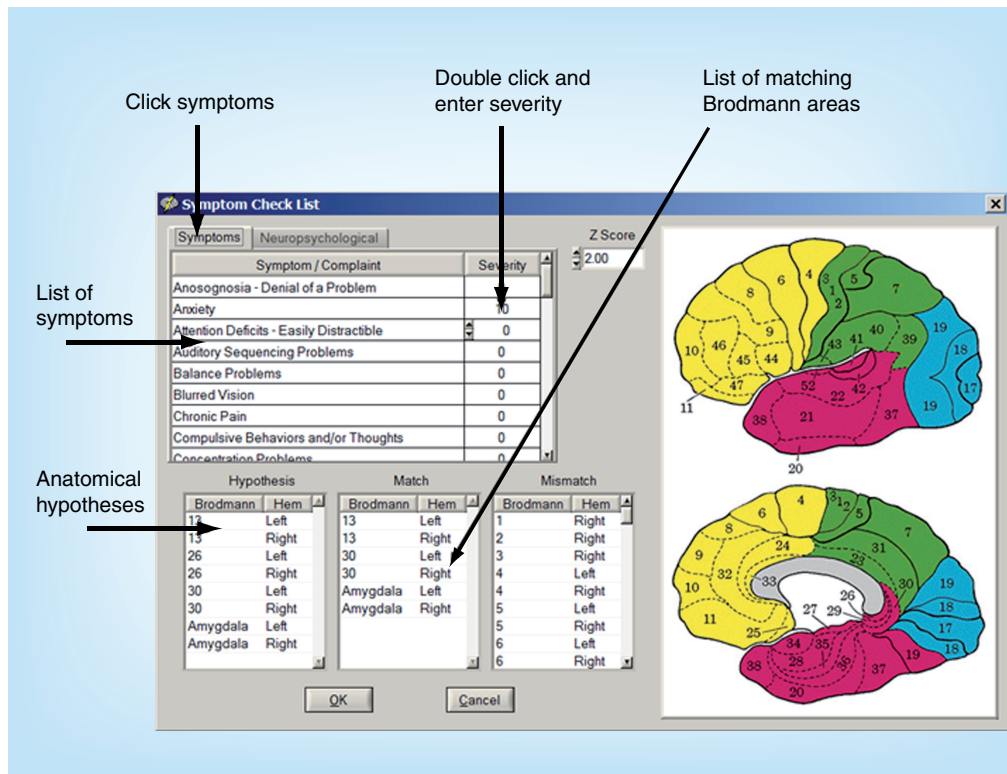
Figure 7. EEG biofeedback of low-resolution electromagnetic tomography Z-scores that are linked to the patient's symptoms and complaints. The upper left panel is a symptom checklist, the right panels are Brodmann areas and the lower left panel is the hypothesized Brodmann areas known to be related to a given symptom or neuropsychological assessment based on the scientific literature. The lower middle panel is the matches of deviant quantitative EEG low-resolution electromagnetic tomography Z-scores to the hypothesized Brodmann areas linked to the patient's symptoms. The lower right panel is the mismatches of deviant low-resolution electromagnetic tomography quantitative EEG Z-scores that are likely related to compensatory processes. The goal of this procedure is to separate the 'weak' systems from the 'compensatory' systems and to target the 'weak' systems for EEG biofeedback training and reinforce movement of the weak system towards $Z = 0$, which is the center of an age-matched normal population. Specific Brodmann areas can be trained, such as the anterior cingulate gyrus in depression or attention deficit, the parahippocampus in attention deficit or the left angular gyurs in dyslexia, among others.

literature to confirm the anatomical linkage to the patient's complaints. In addition to location, electrical neuroimaging provides accurate measures of phase shift and phase lock within and between Brodmann areas that are sufficiently large to be accurately measured using LORETA and other distributed inverse solutions. In the 21st Century, a growing number of neuropsychiatrists will use electrical neuroimaging to help link the patient's symptoms to the time frames of local and distant couplings between Brodmann areas and modules.

In the future, a growing number of pharmaceutical companies will use neuroimaging tools, including qEEG imaging, to develop new medications to better understand the millisecond time domain of the brain (neuromodulators and neurotransmitters, among others). Quantification of medication effects on the brain and the use of EEG biofeedback to modify deregulated neural networks can be synergistic with medication and result in fewer sessions, lower dosages and improved clinical outcomes. Neuropsychiatry faces a bright future and will continue to grow with the benefit of new discoveries in neuroscience and neuroimaging.

Bibliography

Papers of special note have been highlighted as:
■ of interest
■■ of considerable interest

1   Buzsaki G. *Rhythms of the Brain.* Oxford University Press, MA, USA (2006).

2   Hughes JR, John ER. Conventional and quantitative electroencephalography in psychiatry. *J. Neuropsychiatry Clin. Neurosci.* 11(2), 190–208 (1999).

■   **Reviews the relative effect sizes of nonquantitative EEG versus quantitative EEG (qEEG).**

3   John ER. Neurometrics: quantitative electrophysiological analyses. In: *Functional Neuroscience, Volume II.* John ER, Thatcher RW (Eds). L Erlbaum Associates, NJ, USA, 99–174 (1997).

4   Matousek M, Petersen I. Automatic evaluation of background activity by means of age-dependent EEG quotients. *EEG Clin. Neurophysiol.* 35, 603–612 (1973).

5   Matousek M, Petersen I. Frequency analysis of the EEG background activity by means of age dependent EEG quotients. In: *Automation of Clinical Electroencephalography.* Kellaway P, Petersen I (Eds). Raven Press, NY, USA, 75–102 (1973).

6   John ER, Karmel B, Corning W *et al.* Neurometrics: numerical taxonomy identifies different profiles of brain functions within groups of behaviorally similar people. *Science* 196, 1393–1410 (1977).

7   John ER, Prichep LS, Easton P. Normative data banks and neurometrics: basic concepts, methods and results of norm construction. In: *Handbook of Electroencephalography and Clinical Neurophysiology: Volume III. Computer Analysis of the EEG and Other Neurophysiological Signals.* Remond A (Ed.). Elsevier, The Netherlands, 449–495 (1987).

8   John ER, Prichep LS. Principles of neurometric analysis of EEG and evoked potentials. In: *Electroencephalography: Basic Principles, Clinical Applications, and Related Fields (3rd Edition).* Niedermeyer E, Lopes da Silva F (Eds). Williams and Wilkins, MD, USA, 989–1003 (1993).

9   Duffy F, Hughes JR, Miranda F, Bernad P, Cook P. Status of quantitative EEG (qEEG) in clinical practice. *Clin. Electroencephal.* 25(4), VI–XXII (1994).

10 Thatcher RW, Walker RA, Biver C, North D, Curtin R. Quantitative EEG normative databases: validation and clinical correlation. *J. Neurotherapy* 7(3–4), 87–122 (2003).

■■ **Provides systematic cross-validation tests of qEEG normative databases.**

11 Congedo M, Lubar J. *Parametric and Non-Parametric Analysis of QEEG: Normative Database Comparisons in Electroencephalography, A Simulation Study on Accuracy.* Lubar J (Ed.). Haworth Press, NY, USA (2003).

12 Thatcher RW, Lubar JF. History of the scientific standards of qEEG normative databases. In: *Introduction to qEEG and Neurofeedback: Advanced Theory and Applications.* Budzinsky T, Budzinsky H, Evans J, Abarbanel A (Eds). Academic Press, CA, USA, 29–62 (2008).

■■ **Reviews the history of the scientific standards of qEEG normative databases,**

13 Lorensen TD, Dickson P. Quantitative EEG normative databases: a comparative investigation. *J. Neurotherapy* 7(3–4), 53–68 (2003).

14 White JN. Comparison of qEEG reference databases in basic signal analysis and in the evaluation of adult ADHD. *J. Neurotherapy* 7(3–4), 123–169 (2003).

15 Bosch-Bayard J, Valdes-Sosa P, Virues-Alba T *et al.* 3D statistical parametric mapping of EEG source spectra by means of variable resolution electromagnetic tomography (VARETA). *Clin. EEG* 32(2), 47–61 (2001).

16 Narushima K, McCormick LM, Yamada T, Thatcher RW, Robinson RG. Subgenual cingulate θ activity predicts treatment response of repetitive transcranial magnetic stimulation in participants with vascular depression. *J. Neuropsychiatr. Clin. Neurosci.* 22(1), 75–84 (2010).

17 Mobascher A, Brinkmeyer J, Warbrick T *et al.* Fluctuations in electrodermal activity reveal variations in single trial brain responses to painful laser stimuli – a fMRI/EEG study. *Neuroimage* 44(3), 1081–1092 (2009).

18 McCormick LM, Yamada T, Yeh M, Brumm MC, Thatcher RW. Antipsychotic effect of electroconvulsive therapy is related to normalization of subgenual cingulate θ activity in psychotic depression. *J. Psychiatr. Res.* 43(5), 553–560 (2009).

19 Thatcher RW, North D, Biver C. Self organized criticality and the development of EEG phase reset. *Hum. Brain Mapp.* 30(2), 553–574 (2009).

20 Galderisi S, Mucci A, Volpe U, Boutros N. Evidence-based medicine and electrophysiology in schizophrenia. *Clin. EEG Neurosci.* 40(2), 62–77 (2009).

21 Clark CR, Galletly CA, Ash DJ, Moores KA, Penrose RA, McFarlane AC. Evidence-based medicine evaluation of electrophysiological studies of the anxiety disorders. *Clin. EEG Neurosci.* 40(2), 84–112 (2009).

22 Cantor DS, Chabot R. qEEG studies in the assessment and treatment of childhood disorders. *Clin. EEG Neurosci.* 40(2), 113–121 (2009).

23 Lancaster JL, Woldorff MG, Parsons LM, Liotti M, Freitas CS, Rainey L. Automatic Talairach atlas labels for functional brain mapping. *Hum. Brain Mapp.* 10, 120–131 (2000).

24 Michel CM, Koenig T, Brandeis D, Gianotti LR, Waxkerman J. *Electrical Neuroimaging.* Cambridge University Press, NY, USA (2009).

25 Valdes-Sosa P, Valdes-Sosa M, Carballo J *et al.* qEEG in a public health system, *Brain Topogr.* 4(4), 259–266 (1992).

26 Malmivuo J, Plonsey R. *Bioelectromagnetism.* Oxford University Press, UK (1995).

27 Klein M. *Mathematical Thought from Ancient to Modern Times.* Oxford University Press, NY, USA (1972).

28 Hämäläinen MS, Ilmoniemi RJ. Interpreting measured magnetic fields of the brain: estimates of current distributions. *Med. Biol. Eng. Comput.* 32(1), 35–42 (1984).

29 Thatcher R, Wang B, Toro C, Hallett M. Human neural network dynamics using multimodal registration of EEG, PET and MRI. In: *Functional Neuroimaging: Technical Foundations.* Thatcher R,

Hallett M, Zeffiro T, John E, Huerta M (Eds). Academic Press, NY, USA, 269–278 (1994).

30 *Developmental Neuroimaging: Mapping the Development of Brain and Behavior.* Thatcher RW, Lyon GR, Rumsey J, Krasnegor N (Eds). Academic Press, FL, USA (1996).

31 Deuchar DC. An introduction to automated electrocardiogram interpretation. *Proc. R. Soc. Med.* 68(2), 133 (1975).

32 Pilkington TC, Plonsey R. *Engineering Contributions to Biophysical Electrocardiography.* IEEE Press, John Wiley, NY, USA (1982).

33 Wang J, Williamson S, Kauffman L. Magnetic source images determined by lead-field analysis: the unique minimum-norm least squares simulation. *IEEE Trans. Biomed. Eng.* 39, 665–667 (1992).

34 Pascual-Marqui RD, Michel CM, Lehmann D. Low resolution electromagnetic tomography: a new method for localizing electrical activity in the brain. *Int. J. Psychophysiol.* 18, 49–65 (1994).

■■ **Seminal study introducing EEG tomography by the method called 'low-resolution electromagnetic tomography'.**

35 Pascual-Marqui RD. Review of methods for solving the EEG inverse problem. *Int. J. Bioelectromagnetism* 1(1), 75–86 (1999).

36 Galán L, Biscay R, Valdés P *et al.* Multivariate statistical brain electromagnetic mapping. *Brain Topogr.* 7(1), 17–28 (1994).

37 Pascual-Marqui R. Standardized low-resolution brain electromagnetic tomography (sLORETA): technical details. *Methods Find. Exp. Clin. Pharmacol.* 24(Suppl. D), 5–12 (2002).

38 Friston K, Holmes A, Worsley K *et al.* Statistical parametric maps in functional imaging: a general linear approach. *Hum. Brain Mapp.* 2, 189–210 (1994).

39 Thatcher RW, North D, Biver C. EEG inverse solutions and parametric vs. non-parametric statistics of low resolution electromagnetic tomography (LORETA). *Clin. EEG Neurosci.* 36(1), 1–9 (2005).

40 Thatcher RW, North D, Biver C. Evaluation and validity of a LORETA normative EEG database. *Clin. EEG Neurosci.* 36(2), 116–122 (2005).

■■ **Demonstration of the cross-validation accuracy of a normative EEG tomography database.**

41 Hernandez-Gonzalez G, Bringas-Vega ML, Galán-García L, Bosch-Bayard J, Lorenzo-Ceballos Y, Valdes-Sosa PA.

Multimodal quantitative neuroimaging databases and methods: the Cuban Human Brain Mapping Project. *Clin. EEG Neurosci.* 42(3), 1–11 (2011).

■ **Review of the history of EEG tomography normative databases.**

42 Palmero-Soler E, Dolan K, Hadamschek V *et al.* swLORETA: a novel approach to robust source localization and synchronization tomography. *Phys. Med. Biol.* 52, 1783–1794 (2007).

43 Grave de Peralta-Menendez R, Gonzalez-Andino S, Lantz G *et al.* Noninvasive localization of electromagnetic epileptic activity. I. Method descriptions and simulations. *Brain Topogr.* 14(2), 131–137 (2001).

44 Yoo SS, Talos IF, Golby AJ, Black PM, Panych LP. Evaluating requirements for spatial resolution of fMRI for neurosurgical planning. *Hum. Brain Mapp.* 21, 34–43 (2004).

45 Ozcan M, Baumgartner UL, Vucurevic G, Stoeter P, Treede RD. Spatial resolution of fMRI in the human parasylvian cortex: comparison of somatosensory and auditory activation. *Neuroimage* 25, 877–887 (2005).

46 Gomez J, Thatcher RW. Frequency domain equivalence between potentials and currents using LORETA. *Int. J. Neurosci.* 107, 161–171 (2001).

47 Thatcher RW, Biver C, Camacho M, McAlaster R, Salazar AM. Biophysical linkage between MRI and EEG amplitude in traumatic brain injury. *Neuroimage* 7, 352–367 (1998).

48 Thatcher RW, Biver C, McAlaster R, Salazar AM. Biophysical linkage between MRI and EEG coherence in traumatic brain injury. *Neuroimage* 8(4), 307–326 (1998).

49 Thatcher RW, Biver CL, Gomez-Molina JF *et al.* Estimation of the EEG power spectrum by MRI T_2 relaxation time in traumatic brain injury. *Clin. Neurophysiol.* 112, 1729–1745 (2001).

50 Baars BJ. The conscious access hypothesis: origins and recent evidence. *Trends Cogn. Sci.* 6, 47–52 (2002).

51 Peled A. *Neuroanalysis: Bridging the Gap Between Neuroscience, Psychoanalysis, and Psychiatry.* Routledge, UK (2008).

52 Thatcher RW, North D, Biver C. Intelligence and EEG phase reset: a two-compartmental model of phase shift and lock. *Neuroimage* 42(4), 1639–1653 (2008).

53 Varela FJ. Resonant cell assemblies: a new approach to cognitive functions and neuronal synchrony. *Biol. Res.* 28(1), 81–95 (1995).

54 Sauseng P, Klimesch W. What does phase information of oscillatory brain activity tell us about cognitive processes? *Neurosci. Biobehav. Rev.* 32(5), 1001–1013 (2008).

55 Singer W. Development and plasticity of cortical processing architectures. *Science* 270, 758–764 (1995).

56 Nadasdy Z. Binding by asynchrony: the neuronal phase code. *Front. Neurosci.* 4(51), 1–10 (2010).

57 Freeman WJ, Rogers LJ. Fine temporal resolution of analytic phase reveals episodic synchronization by state transitions in γ EEGs. *J. Neurophysiol.* 87(2), 937–945 (2002).

58 Freeman WJ, Burke BC, Homes MD. A periodic phase re-setting in scalp EEG of β–γ oscillations by state transitions at α–θ rates. *Hum. Brain Mapp.* 19(4), 248–272 (2003).

59 Breakspear M. Terry JR. Detection and description of non-linear interdependence in normal multichannel human EEG data. *Clin. Neurophysiol.* 113(5), 735–753 (2002).

60 Breakspear M. Terry JR. Nonlinear interdependence in neural systems: motivation, theory and relevance. *Int. J. Neurosci.* 112(10), 1263–1284 (2002).

61 Lachaux JP, Rodriguez E, Le Van Quyen M, Lutz A, Martinerie J, Varela FJ. Studying single-trials of phase synchronous activity in the brain. *Int. J. Bifuc. Chaos* 10(10), 2429–2439 (2000).

62 Thatcher RW, North D, Neurbrander J, Biver CJ, Cutler S, DeFina P. Autism and EEG phase reset: deficient GABA mediated inhibition in thalamo–cortical circuits. *Dev. Neuropsych.* 34(6), 780–800 (2009).

63 Luria A. *The Working Brain: an Introduction to Neuropsychology.* Penguin Books, MD, USA (1973).

64 Mesulam M. *Principles of Behavioral and Cognitive Neurology (2nd Edition)*, Oxford University Press, MA, USA (2000).

65 Hagmann P, Cammoun L, Gigandet X *et al.* Mapping the structural core of human cerebral cortex. *PLoS Biol.* 6, E159 (2008).

66 Chen ZJ, He Y, Rosa-Neto P, Germann J, Evans AC. Revealing modular architecture of human brain structural networks by using cortical thickness from MRI. *Cereb. Cortex* 18, 2374–2381 (2008).

67 He Y, Wang J, Wang L *et al.* Uncovering intrinsic modular organization of spontaneous brain activity in humans. *PLoS One* 4(4), E5226 (2009).

68 Langer N, Pedroni A, Gianotti AR, Hanggi J, Knoch D, Jancke L. Functional brain network efficiency predicts intelligence human

brainmapping. *Hum. Brain Mapp.* doi: 10.1002/hbm.21297 (2011) (Epub ahead of print).

69 Damoiseaux JS, Smith SM, Witter MP *et al.* White matter tract integrity in aging and Alzheimer's disease. *Hum. Brain Mapp.* 30, 1051–1059 (2009).

70 Netoff TI. Schiff SJ. Decreased neuronal synchronization during experimental seizures. *J. Neurosci.* 22(16), 7297–7307 (2002).

71 Rami L, Gómez-Anson B, Monte GC, Bosch B, Sánchez-Valle R, Molinuevo JL. Voxel based morphometry features and follow-up of amnestic patients at high risk for Alzheimer's disease conversion. *Int. J. Geriatr. Psychiatr.* 24, 875–884 (2009).

72 Zhou J, Greicius MD, Gennatas ED *et al.* Divergent network connectivity changes in behavioural variant frontotemporal dementia and Alzheimer's disease. *Brain* 133, 1352–1367 (2010).

73 Mobascher A, Brinkmeyer J, Warbrick T *et al.* Laser-evoked potential P2 single-trial amplitudes covary with the fMRI BOLD response in the medial pain system and interconnected subcortical structures. *Neuroimage* 45(3), 917–926 (2009).

74 Esposito F, Mulert C, Goebel R. Combined distributed source and single-trial EEG–fMRI modeling: application to effortful decision making processes. *Neuroimage* 47(1), 112–121 (2009).

75 Esposito F, Aragri A, Piccoli T, Tedeschi G, Goebel R, Di Salle F. Distributed analysis of simultaneous EEG–fMRI time-series: modeling and interpretation issues. *Magnet. Resonance Imaging* 27(8), 1120–1130 (2009).

76 Brookings T, Ortigue S, Grafton S, Carlson J. Using ICA and realistic BOLD models to obtain joint EEG/fMRI solutions to the problem of source localization. *Neuroimage* 44(2), 411–420 (2009).

77 Yoshioka T, Toyama K, Kawato M *et al.* Evaluation of hierarchical Bayesian method through retinotopic brain activities reconstruction from fMRI and MEG signals. *Neuroimage* 42(4), 1397–1413 (2008).

78 Schulz E, Maurer U, van der Mark S *et al.* Impaired semantic processing during sentence reading in children with dyslexia: combined fMRI and ERP evidence. *Neuroimage* 41(1), 153–168 (2008).

79 Horacek J, Brunovsky M, Novak T *et al.* Effect of low-frequency rTMS on electromagnetic tomography (LORETA) and regional brain metabolism (PET) in schizophrenia patients with auditory hallucinations. *Neuropsychobiology* 55(3–4), 132–142 (2007).

80 Hu J, Tian J, Yang L, Pan X, Liu J. Combination of PCA and LORETA for sources analysis of ERP data: an emotional processing study. Presented at: *Medical Imaging 2006: Physiology, Function, and Structure from Medical Images.* San Diego, CA, USA, 12 February 2006.

81 Zumsteg D, Wennberg RA, Treyer V, Buck A, Wieser HG. H$_2$^{15}O or ^{13}NH$_3$ PET and electromagnetic tomography (LORETA) during partial status epilepticus. *Neurology* 65(10), 1657–1660 (2005).

82 Tišlerová B, Horácek J, Brunovský M, Kopecek M. ^{18}FDG PET and qEEG imaging of hebephrenic schizophrenia. A case study. Hebefrenní schizofrenie v obraze ^{18}FDG PET a qEEG. *Kazuistika* 9(2), 144–149 (2005).

83 Kopecek M, Brunovský M, Bareš M *et al.* Regional cerebral metabolic abnormalities in individual patients with nonquantitative ^{18}FDG PET and qEEG (LORETA). *Psychiatrie* 9(Suppl. 3), 56–63 (2005).

84 Korn A, Golan H, Melamed I, Pascual-Marqui R, Friedman A. Focal cortical dysfunction and blood–brain barrier disruption in patients with postconcussion syndrome. *J. Clin. Neurophysiol.* 22(1), 1–9 (2005).

85 Cannon R, Congredo M, Lubar J, Hutchens T. Differentiating a network of executive attention: LORETA neurofeedback in anterior cingulate and dorsolateral prefrontal cortices. *Int. J. Neurosci.* 119(3), 404–441 (2009).

86 Cannon R, Lubar J, Gerke A, Thornton K, Hutchens T, McCammon V. EEG spectral-power and coherence: LORETA neurofeedback training in the anterior cingulate gyrus. *J. Neurotherapy* 10(1), 5–31 (2006).

87 Cannon R, Lubar JF, Congedo M *et al.* The effects of neurofeedback training in the cognitive division of the anterior cingulate gyrus. *Int. J. Sci.* 117(3), 337–357 (2007).

88 Cannon R, Lubar J, Thornton K, Wilson S, Congedo M. Limbic β activation and LORETA: can hippocampal and related limbic activity be recorded and changes visualized using LORETA in an affective memory condition? *J. Neurotherapy* 8(4), 5–24 (2005).

89 Cannon R, Lubar J. EEG spectral power and coherence: differentiating effects of spatial-specific neuro-operant learning (SSNOL) utilizing LORETA neurofeedback training in the anterior cingulate and bilateral dorsolateral prefrontal cortices. *J. Neurotherapy* 11(3), 25–44 (2007).

90 Cannon R, Lubar J, Sokhadze E, Baldwin D. LORETA neurofeedback for addiction and the possible neurophysiology of psychological processes influenced: a case study and region of interest analysis of LORETA neurofeedback in right anterior cingulate cortex. *J. Neurotherapy* 12(4), 227–241 (2008).

91 Congedo M, Lubar J, Joffe D. Low-resolution electromagnetic tomography neurofeedback. *IEEE Trans. Neural Syst. Rehabil. Eng.* 12, 387–397 (2004).

92 Lubar J, Congedo M. Askew JH. Low-resolution electromagnetic tomography (LORETA) of cerebral activity in chronic depressive disorder. *Int. J. Psychophysiol.* 49(3), 175–185 (2003).

93 deCharms RC. Applications of real-time fMRI. *Nat. Neurosci.* 9, 720–729 (2008).

94 Ilmoniemi RJ, Kicic D. Methodology for combined TMS and EEG. *Brain Topogr.* 22, 233–248 (2010).

95 Pell SG, Roth Y, Zangen A. Modulation of cortical excitability induced by repetitive transcranial magnetic stimulation: influence of timing and geometrical parameters and underlying mechanisms. *Prog. Neurobiol.* 93, 59–98 (2010).

96 Malmivuo JA, Suihko VE. Effect of skull resistivity on the spatial resolutions of EEG and MEG. *IEEE Trans. Biomed. Eng.* 51(7), 1276–1280 (2004).

97 Hansen PC, Kringelback ML, Salmelin R. *MEG: an Introduction to Methods.* Oxford University Press, NY, USA (2010).

98 Srinivasan R, Winter WR, Ding J, Nunez PL. EEG and MEG coherence: measures of functional connectivity at distinct spatial scales of neocortical dynamics. *J. Neurosci. Methods* 166(1), 41–52 (2008).

99 Le Van Quyen M. Disentangling the dynamic core: a research program for a neurodynamics at the large-scale. *Biol. Res.* 36, 67–88 (2003).

100 Hughes SW, Crunelli V. Just a phase they're going through: the complex interaction of intrinsic high-threshold bursting and gap junctions in the generation of thalamic α and θ rhythms. *Int. J. Psychophysiol.* 64, 3–17 (2007).

101 Hughes SW, Lörincz M, Cope DW *et al.* Synchronized oscillations at α and θ frequencies in the lateral geniculate nucleus. *Neuron* 42, 253–268 (2004).

102 Ko TW, Ermentrout GB. Effects of axonal time delay on synchronization and wave formation in sparsely coupled neuronal oscillators. *Phys. Rev. E Stat. Nonlin. Soft Matter Phys.* 76(5 Pt 2), 056206 (2007).

103 Sherman A, Rinzel J. Rhythmogenic effects of weak electrotonic coupling in neuronal models. *Proc. Natl Acad. Sci. USA* 89, 2471–2474 (1992).

104 Sherman A. Anti-phase, asymmetric and aperiodic oscillations in excitable cells – I. Coupled bursters. *Bull. Math. Biol.* 56, 811–835 (1994).

105 Bem T, Rinzel J. Short duty cycle destabilizes a half-center oscillator, but gap junctions can restabilize the anti-phase pattern. *J. Neurophysiol.* 91, 693–703 (2004).

106 Stam CJ, de Bruin EA. Scale-free dynamics of global functional connectivity in the human brain. *Hum. Brain Mapp.* 22, 97–109 (2004).

107 Sporns O, Chialvo D, Kaiser M, Hilgetag CC. Organization, development and function of complex brain networks. *Trends Cogn. Sci.* 8, 418–425 (2004).

108 Breakspear M, Terry JR. Detection and description of non-linear interdependence in normal multichannel human EEG data. *Clin. Neurophysiol.* 113(5), 735–753 (2002).

109 Breakspear M, Terry JR. Nonlinear interdependence in neural systems: motivation, theory and relevance. *Int. J. Neurosci.* 112(10), 1263–1284 (2002).

110 Rudrauf D, Douiri A, Kovach C *et al.* Frequency flows and the time–frequency dynamics of multivariate phase synchronization in brain signals. *Neuroimage* 31, 209–227 (2006).

111 Scannell JW, Burns GA, Hilgetag CC, O'Neil MA, Young MP. The connectional organization of the cortico–thalamic system of the cat. *Cereb. Cortex* 9 277–299 (1999).

112 Bullmore E, Sporns O. Complex brain networks: graph theoretical analysis of structural and functional systems. *Nat. Rev. Neurosci.* 10(3), 186–198 (2009).

113 Achard S, Bullmore E. Efficiency and cost of economical brain functional networks. *PLoS Comput. Biol.* 3, E17 (2007).

114 Stam CJ, Jones BF, Nolte G, Breakspear M, Scheltens P. Small-world networks and functional connectivity in Alzheimer's disease. *Cereb. Cortex* 17(1), 92–99 (2007).

115 Lopes Da Silva FH, Pijn JP. *Handbook of Brain Theory and Neural Networks.* MIT Press, MA, USA (1995).

116 Le Van Quyen M, Martinerie J, Navarro V, Varela FJ. Characterizing neurodynamic changes before seizures. *J. Clin. Neurophysiol.* 18(3), 191–208 (2001).

117 Chavez M, Le Van Quyen M, Navarro V, Baulac M, Martinerie J. Spatio–temporal dynamics prior to neocortical seizures: amplitude versus phase couplings. *IEEE Trans. Biomed. Eng.* 50(5), 571–583 (2003).

118 Stam CJ, van der Made Y, Pijnenburg YAL, Scheltens PH. EEG synchronization in mild cognitive impairment and Alzheimer's disease. *Acta Neurol. Scand.* 106, 1–7 (2002).

119 Stam CJ, van Cappellen van Walsum AM, Pijnenburg YAL *et al.* Generalized synchronization of MEG recordings in Alzheimer's disease: evidence for involvement of the γ band. *J. Clin. Neurophysiol.* 19, 562–574 (2002).

120 Sponheim SR, McGuire KA, Kang SS *et al.* Evidence of disrupted functional connectivity in the brain after combat-related blast injury. *Neuroimage* 54, S21–S29 (2010).

121 Kahana MJ. The cognitive correlates of human brain oscillations. *J. Neurosci.* 26, 1669–1672 (2006).

122 Kirschfeld K. The physical basis of α waves in the electroencephalogram and the origin of the 'Berger effect'. *Biol. Cybem.* 92(3), 177–185 (2005).

123 Tesche CD, Karhu J. θ oscillations index human hippocampal activation during a working memory task. *Proc. Natl Acad. Sci. USA* 97(2), 919–924 (2000).

124 John ER. Mechanisms of memory. *Science* 160, 1097–1099 (1968).

125 Rizzuto DS, Madsen JR, Bromfield EB *et al.* Reset of human neocortical oscillations during a working memory task. *Proc. Natl Acad. Sci. USA* 100(13), 7931–7936 (2003).

126 Damasio AR. Time-locked multiregional retroactivation: a systems-level proposal for the neural substrates of recall and recognition. *Cognition* 33, 25–62 (1989).

127 Tallon-Baudry C, Bertrand O, Fischer C. Oscillatory synchrony between human extrastriate areas during visual short-term memory maintenance. *J. Neurosci.* 21(20), RC177 (2001).

128 Vaadia E, Haalman L, Abeles M *et al.* Dynamics of neuronal interactions in monkey cortex in relation to behavior events. *Nature* 373(6514), 515–518 (1995).

129 Roelfsmem PR, Engel AK, Konig P, Singer W. Visuomotor integraton is associated with zero time-lag synchronization among cortical areas. *Nature* 385(6612), 157–161 (1997).

130 McCartney H, Johnson AD, Wei, ZM, Givens B. θ reset produces optimal conditions for long-term potentiation. *Hippocampus* 14(6), 684–697 (2004).

131 Baars BJ. The conscious access hypothesis: origins and recent evidence. *Trends Cogn. Sci.* 6, 47–52 (2002).

132 Cosmelli D, David O, Lachaux JP *et al.* Waves of consciousness: ongoing cortical patterns during binocular rivalry. *Neuroimage* 23(1), 128–140 (2004).

133 Varela FJ, Lachaux JP, Rodriguez E, Martinerie J. The brainweb: phase synchronization and large-scale integration. *Nat. Rev. Neurosci.* 2(4), 229–239 (2001).

134 John ER. The neurophysics of consciousness. *Brain Res. Brain Res. Rev.* 39(1), 1–28 (2002).

135 John ER. From synchronous neural discharges to subjective awareness? *Prog. Brain Res.* 150, 143–171 (2005).

136 Achard S, Salvador R, Whitcher B, Suckling J, Bullmore E. A resilient, low-frequency, small-world human brain functional network with highly connected association cortical modules. *J. Neurosci.* 26, 63–72 (2006).

137 Teipel SJ, Pogarell O, Meindl T *et al.* Regional networks underlying interhemispheric connectivity: an EEG and DTI study in healthy ageing and amnestic mild cognitive impairment. *Hum. Brain Mapp.* 30(7), 2098–2119 (2009).

138 Lee WH, Kim TS, Kim AT, Lee SY. 3-D diffusion tensor MRI anisotropy content-adaptive finite element head model generation for bioelectromagnetic imaging. *IEEE Eng. Med. Biol. Soc.* 4003–4006 (2008).

139 Brodmann VK. *Localization in the Cerebral Cortex: the Principles of Comparative Localisation in the Cerebral Cortex Based on Cytoarchitectonics.* Garey LJ (Ed.). Springer, UK (1994).

140 Towle VL, Bolanos J, Suarez D *et al.* The spatial location of EEG electrodes: locating the best-fitting sphere relative to cortical anatomy. *Electroencephal. Clin. Neurophysiol.* 86, 1–6 (1993).

141 Pascual-Marqui RD, Koukkou M, Lehmann D, Kochi, K. Functional localization and functional connectivity with LORETA comparison of normal controls and first episode drug naive schizophrenics. *J. Neurotherapy* 4(4), 35–37 (2001).

142 Thut G. Pascual-Leone AA. Review of combined TMS–EEG studies to characterize lasting effects of repetitive TMS and assess their usefulness in cognitive and clinical neuroscience. *Brain Topogr.* 22, 219–232 (2010).

143 Stam CJ, de Haan W, Daffertshofer A *et al.* Graph theoretical analysis of magnetoencephalographic functional connectivity in Alzheimer's disease. *Brain* 132, 213–224 (2009).

144 Hoechstetter K, Bornfleth H, Weckesser D, Ille N, Berg P, Scherg M. BESA source coherence: a new method to study cortical oscillatory coupling. *Brain Topogr.* 16, 233–238 (2004).

145 Thatcher RW. Tomographic EEG/MEG. *J. Neuroimaging* 5, 35–45 (1995).

146 Thatcher RW, North DM, Biver CJ. Diffusion tensor imaging 'modules' correlated with LORETA electrical neuroimaging 'modules'. *Hum. Brain Mapp.* doi: 10.1002/hbm.21271 (2011) (Epub ahead of print).
■■ **EEG tomography cross-validation with respect to MRI diffusion tensor imaging.**

147 Lehmann D, Faber PL, Gianotti LRR, Kochi K, Pascual-Marqui RD. Coherence and phase locking in the scalp EEG and between LORETA model sources, and microstates as putative mechanisms of brain temporo–spatial functional organization. *J. Physiol.* 99, 29–36 (2006).

148 Thatcher RW, Biver CJ, North D. Spatial–temporal current source correlations and cortical connectivity. *Clin. EEG Neurosci.* 38(1), 35–48 (2007).
■ **Demonstration of cortico–cortical connectivity of Brodmann areas and 3D regions of interest.**

149 Braitenberg V. Cortical architectonics: general and areal. In: *Architectonics of the Cerebral Cortex.* Brazier MAB, Petsche H (Eds). Raven Press, NY, USA, 443–465 (1978).

150 Braitenberg V, Schüz A. *Cortex: Statistics and Geometry of Neuronal Connections (2nd Edition)*. Springer, Germany (1998).

151 Sholl DA. A comparative study of the neuronal packing density in the cerebral cortex. *J. Anat.* 93, 143–158 (1959).

152 Binzegger T, Douglas RJ, Martin KA. An axonal perspective on cortical circuits. In: *New Aspects of Axonal Structure.* Feldmeyer D, Lubkep JHR (Eds). Springer, NY, USA, 117–140 (2010).

153 Schulz A, Braintenberg V. The human cortical white matter: quantitative aspects of cortico–cortical long-range connectivity. In: *Cortical Areas: Unity and Diversity.* Schultz A, Miller R (Eds). Conceptual Advances in Brain Research, UK, 377–386 (2002).

154 Nunez P. *Electrical Fields of the Brain*. Oxford University Press, MA, USA (1981).

155 Nunez P. *Neocortical Dynamics and Human EEG Rhythms*. Oxford University Press, NY, USA (1995).

156 Wangler S, Gevensleben H, Albrecht B *et al.* Neurofeedback in children with ADHD: specific event-related potential findings of a randomized controlled trial. *Clin. Neurophysiol.* 122, 942–950 (2011).

157 Arns M, de Ridder S, Strehl U, Breteler M, Coenen A. Efficacy of neurofeedback treatment in ADHD: the effects on inattention, impulsivity and hyperactivity: a meta-analysis. *Clin. EEG Neurosci.* 40(3), 180–189 (2009).

158 Collura TF, Thatcher RW, Smith ML, Lambos WA, Stark CR. EEG biofeedback training using live Z-scores and a normative database. In: *Introduction to QEEG and Neurofeedback: Advanced Theory and Applications.* Budzinsky T, Budzinsky H, Evans J, Abarbanel A (Eds). Academic Press, CA, USA, 22–33 (2008).

159 Collura TF, Guan J, Tarrant J, Bailey J, Starr F. EEG biofeedback case studies using live Z-score training and a normative database. *J. Neurotherapy* 14, 22–46 (2010).

160 Thatcher RW. EEG operant conditioning (biofeedback) and traumatic brain injury. *Clin. EEG* 31(1), 38–44 (2000).

161 Scherg M, von Cramon D. *Dipole Source Potentials of the Auditory Cortex in Normal Subjects and Patients with Temporal Lobe Lesions, Advances in Audiology, Auditory Evoked Magnetic Fields and Electric Potentials*. Hoke GF, Romani M (Eds). Karger, Switzerland, 165–193 (1990).

162 Mosher J, Baillet S, Leahy R. EEG source localization and imaging using multiple signal classification approaches. *J. Clin. Neurophysiol.* 16(3), 225–238 (1999).

163 Leahy RM, Mosher JC, Spencer ME *et al.* A study of dipole localization accuracy for MEG and EEG using a human skull phantom. *Electroencephal. Clin. Neurophysiol.* 107(2), 159–173 (1998).

164 Uutela K, Hämäläinen M, Somersalo E. Visualization of magnetoencephalographic data using minimum current estimates. *Neuroimage* 10(2), 173–180 (1999).

165 Gorodnitsky I, George J, Rao B. Neuromagnetic source imaging with FOCUSS: a recursive weighted minimum norm algorithm. *Electroencephal. Clin. Neurophysiol.* 95(4), 231–251 (1995).

166 Vega-Hernández M, Martínez-Montes E, Sanchez-Bornot J *et al.* Penalized least squares methods for solving the EEG inverse problem. *Statistica Sinica* 18(4), 1535–1551 (2008).

167 Bourbaki N. *Topological Vector Spaces: Elements of Mathematics*. Springer-Verlag, Germany (1987).

168 Le Van Quyen M. The brainweb of cross-scale interactions. *New Ideas Psychol.* 29, 57–63 (2010).

■ **Websites**

201 Pubmed Homepage
www.ncbi.nlm.nih.gov/sites/entrez?db=pubmed

202 Papers that quote 'Pascual-Marqui RD, Michel CM, Lehmann D: Low resolution electromagnetic tomography: a new method for localizing electrical activity in the brain. *Intl J. Psychophysiology* 18, 49–65 (1994)'
www.uzh.ch/keyinst/NewLORETA/QuoteLORETA/PapersThatQuoteLORETA05.htm